Machine Unlearning in 3D Generation: A Perspective-Coherent Acceleration Framework

Shixuan Wang **Jingwen Ye*** **Xinchao Wang***
National University of Singapore
e1352854@u.nus.edu, {jingweny, xinchao}@nus.edu.sg

Abstract

Recent advances in generative models trained on large-scale datasets have enabled high-quality 3D synthesis across various domains. However, these models also raise critical privacy concerns. Unlike 2D image synthesis, where risks typically involve the leakage of visual features or identifiable patterns, 3D generation introduces additional challenges, as reconstructed shapes, textures, and spatial structures may inadvertently expose proprietary designs, biometric data, or other sensitive geometric information. This paper presents the first exploration of machine unlearning in 3D generation tasks. We investigate different unlearning objectives, including re-targeting and partial unlearning, and propose a novel framework that does not require full supervision of the unlearning target. To enable a more efficient unlearning process, we introduce a skip-acceleration mechanism, which leverages the similarity between multi-view generated images to bypass redundant computations. By establishing coherence across viewpoints during acceleration, our framework not only reduces computation but also enhances unlearning effectiveness, outperforming the non-accelerated baseline in both accuracy and efficiency. We conduct extensive experiments on the typical 3D generation models (Zero123 and Zero123XL), demonstrating that our approach achieves a 30% speedup, while effectively unlearning target concepts without compromising generation quality. Our framework provides a scalable and practical solution for privacy-preserving 3D generation, ensuring responsible AI deployment in real-world applications. The code is available at: https://github.com/sxxsxw/Fast-3D-Unlearn-with-Skip-acceleration

1 Introduction

The ability to generate realistic and diverse 3D content is crucial for applications in gaming, film production, virtual reality, and digital design, where high-quality 3D assets are in high demand. To address this need, 3D generation models Wang et al. [2025], Nash et al. [2020], Raj et al. [2023] have become a key research focus in computer vision and graphics, aiming to automate the creation of detailed and structured 3D representations.

Despite significant advancements, 3D generation also introduces pressing privacy concerns. Many models, particularly large-scale 3D generative foundation models Liu et al. [2023a], Tang et al. [2024], are trained on extensive datasets, increasing the risk of incorporating proprietary, sensitive, or personally identifiable information. This can lead to potential data leakage or unauthorized content reproduction. Additionally, generative 3D models may inadvertently expose intricate details of objects, raising ethical and legal challenges. Addressing these privacy risks is critical for the responsible development and deployment of 3D generation technologies, yet it remains an underexplored issue.

*Corresponding authors

39th Conference on Neural Information Processing Systems (NeurIPS 2025).

Figure 1: Given a single input image, the target Image-to-3D model generates a multi-view representation of the object. Our proposed framework applies an unlearning process to the target model, enabling tasks such as stylization removal, partial unlearning, and retargeting.

Over the past few years, the community has increasingly recognized the importance of ensuring trust and safety in modern generative models. In particular, there is growing interest in developing efficient unlearning methods to remove private or sensitive information from trained models. Given the high cost of retraining large-scale generative models, machine unlearning aims to selectively erase the influence of specific data without requiring full model retraining. Recently, Seo et al. Seo et al. [2024] introduced GUIDE, a framework designed to prevent the reconstruction of a specific identity by unlearning the generator using only a single image. Their approach demonstrates the effectiveness of generative machine unlearning, highlighting the feasibility of targeted knowledge removal.

Despite recent advancements in machine unlearning for image generation, little to no work has explored its application in 3D generation. We argue that trust and safety concerns in 3D generation are just as critical, yet they introduce unique challenges compared to 2D generation. First, since 3D generation involves multi-view image outputs, correcting or modifying specific targets requires consistency across all viewpoints, significantly increasing annotation complexity. Second, unlearning must be applied to each generated view, making the process computationally expensive and time-consuming. These challenges highlight the need for efficient and scalable unlearning techniques tailored to 3D generation.

In this work, we propose the first 3D unlearning framework, targeting zero-shot image-to-3D view synthesis models. These large-scale models, trained on vast datasets, pose increased privacy risks. Our goal is to unlearn a specific object while preserving the generation performance for other objects. To achieve this, we leverage the inherent similarity between different viewpoints, reconstructing unseen views using only the nearest few. Additionally, we introduce an efficient caching mechanism for the diffusion process of key views, significantly accelerating the denoising process for the input object. The unlearning tasks in 3D include changing the style, retargeting to a completely new object, or partially editing the given object. We demonstrate several cases solved by our framework in Fig. 1.

In conclusion, for machine unlearning in 3D tasks, our contributions could be concluded as:

- First, we pioneer the exploration of unlearning in image-to-3D models, addressing the removal of entire objects, specific views, and the style of 3D objects.
- Second, we propose an accelerated unlearning process for image-to-3D models, demonstrating that full supervision with all target object views is unnecessary, making our approach more practical for real-world applications.
- Lastly, we conduct various unlearning experiments in 3D tasks, and our methods maintain the generative quality while achieving 30% speedup.

2 Related Work

2.1 3D Generative Models and Acceleration Techniques

In the past few years, 3D generation has gained significant attention, whose methods including point clouds Bello et al. [2020], Wu et al. [2019], Achlioptas et al. [2018], voxels Liu et al. [2020], Ren et al. [2024], meshes Tsalicoglou et al. [2024], Guédon and Lepetit [2024], Wu et al. [2024a], and implicit fields Sun et al. [2024], Deng et al. [2021]. However, these methods often lack generalization, as they are typically designed for generating specific categories. To overcome this limitation, many

researchers have focused on large-scale 3D generation frameworks trained on extensive 3D datasets. Specifically, a line of research aims to directly learn single-shot novel view generation models conditioned on camera viewpoints from large-scale 3D datasets. For example, Zero123 Liu et al. [2023a] is proposed as a framework for changing the camera viewpoint of an object given just a single RGB image. Following this work, Objaverse-XL Deitke et al. [2023] utilizes over 100 million multiview rendered images for training, thus achieving strong zero-shot generalization abilities. Magic123 Qian et al. [2023] is presented as a two-stage coarse-to-fine approach for high-quality, textured 3D meshes generations with both 2D and 3D priors.

Generative tasks often rely on diffusion models, which involve computationally intensive sampling processes. As a result, recent research has focused on accelerating the generation process Ma et al. [2024], Huang et al. [2025], Yao et al. [2025], So et al. [2023]. For example, Ma et al. Ma et al. [2024] propose the DeepCache framework as a novel training-free paradigm to accelerate diffusion models from the perspective of model architecture. And S^2-DMs Wang and Li [2024] utilizes the accelerating mechanism to reintegrate the information omitted during the selective sampling phase. This challenge is even more pronounced in 3D generation, where optimization typically requires tens of thousands of iterations of full-image volume rendering and prior model inferences, often taking tens of minutes per shape. To improve efficiency, numerous studies Liu et al. [2023b], Shi et al. [2023], Liu et al. [2023c], Li et al. [2023], Liu et al. [2024a] have explored ways to accelerate both training and reconstruction. For instance, One-2-3-45 Liu et al. [2023b] utilizes multi-view images predicted by Zero123 to generate a textured 3D mesh in just 45 seconds, while One-2-3-45++ Liu et al. [2023c] enhances texture quality through lightweight optimization. In contrast to these acceleration-focused methods, our framework is designed for unlearning, aiming to efficiently remove the influence of specific views or concepts.

2.2 Machine Unlearning

The concept of machine unlearning is firstly introduced by Bourtoule et al. Bourtoule et al. [2021], which aims to eliminate the effect of data point(s) on the already trained model without retraining the model from scratch. In the past few years, it has been well studied especially in classification tasks Tarun et al. [2023], Ye et al. [2022], Kurmanji et al. [2023]. However, these approaches face scalability challenges in generative tasks due to the massive training datasets and the large model sizes involved.

Since large-scale models are trained on extensive datasets, they often raise privacy concerns, prompting increasing research efforts to address these issues Liu et al. [2025], Shi et al. [2024], Li et al. [2025], Liu et al. [2024b]. For instance, Liu et al.Liu et al. [2025] investigate machine unlearning in large language models (LLMs), aiming to remove sensitive or illegal information while preserving essential knowledge and model capabilities. In diffusion models, Wu et al.Wu et al. [2024b] propose aligning the output domains of sensitive and anchor concepts through adversarial training, while meta-unlearning Gao et al. [2024] not only removes harmful or copyrighted concepts but also prevents their malicious relearning. Additionally, Score Forgetting Distillation (SFD) Chen et al. [2024] accelerates forgetting while preserving generation quality and improving inference speed. Our work further enriches this field by being the first to explore unlearning in 3D generation, extending the scope of machine unlearning to address ethical concerns in generative AI.

3 Methods

3.1 Problem Formulation

Our target model is a zero-shot image-to-3D view synthesis model f, which generates multi-view 3D representations from a single image. Recall that in the 2D setting, unlearning aims to remove specific objects or attributes from a pre-trained generative model while preserving its ability to generate other realistic images. Given a diffusion-based generative model f, which generates images from noise z, such unlearning modifies the model to ensure that a target object I_t is removed while maintaining overall generation quality:

$$\tilde{x} = f_u(z, \phi), \quad \text{s.t.} \quad \tilde{x} \not\approx I_t, \tag{1}$$

where f_u represents the unlearned model for the target object. The main challenge in 2D unlearning lies in selectively forgetting the exact object without affecting unrelated generations. Since image

synthesis occurs in a single 2D space, this process is computationally feasible using methods such as gradient-based fine-tuning or regularization-based memory erasure.

3D generation models, such as zero-shot image-to-3D synthesis models f, are typically trained to learn a mapping from a single input image I to a set of novel viewpoints for 3D reconstruction:

$$\mathcal{X} = \{x(\theta) \mid x(\theta) = f(I, \theta)\}, \tag{2}$$

where $x(\theta)$ denotes the synthesized image from viewpoint θ. These models are often trained on large-scale datasets and may inadvertently memorize information from the training data, leading to potential privacy risks.

Unlike 2D unlearning, where modifications are applied to a single image, 3D unlearning must ensure that the target object is removed across multiple viewpoints. This requires updating the model f across the full set of angles Θ, leading to significantly higher computational cost:

$$\ell_{\text{unlearn}} = \sum_{\theta \in \Theta} |f_u(I, \theta) - \tilde{x}(\theta)|^2. \tag{3}$$

where $\tilde{x}(\theta)$ is the target image with the sensitive content removed at viewpoint θ. Since diffusion-based 3D models generate each view iteratively, this increases the overall training cost by a factor of $|\Theta|$, where $|\Theta|$ is the number of sampled viewpoints.

Our goal is to develop an **efficient** 3D unlearning framework that removes specific objects or attributes (donated as the forget set D_f) from the target model f while preserving its ability to generate accurate 3D views of other objects (donated as the preservation set D_r). To achieve this, we propose a **dynamic skipping scheme** (Sec. 3.2) that accelerates the 3D unlearning process by strategically leveraging multi-view consistency, reducing redundant computations while maintaining coherence across viewpoints. Throughout the rest of the paper, we use the re-targeting task as an illustrative example of our approach. Specifically, we aim to adapt the generation results for the forget set $\mathcal{D}_f$ so that they resemble those of a designated re-target set $\mathcal{D}_o$. This objective is formalized as:

$$\{f_u(I, \theta) \mid I \in \mathcal{D}_f\} \approx \{f(I, \theta) \mid I \in \mathcal{D}_o\}, \quad \{f_u(I, \theta) \mid I \in \mathcal{D}_r\} \approx \{f(I, \theta) \mid I \in \mathcal{D}_r\}, \tag{4}$$

where f_u denotes the updated model after unlearning, and the goal is to make the outputs of f_u on $\mathcal{D}_f$ indistinguishable from those on $\mathcal{D}_o$.

3.2 Dynamic Skipping via Interpolation

To address the high computational cost of 3D unlearning across dense viewpoints, we introduce a **dynamic skipping scheme**. Instead of independently unlearning each view, our method strategically selects a sparse set of key viewpoints and interpolates the remaining ones. By leveraging multi-view consistency, this approach significantly reduces redundant updates while preserving visual coherence across views.

For each selected key view $\theta_s \in \Theta$, the reverse diffusion process is performed iteratively over T steps. At each step, the model refines the latent representation by removing a portion of the noise, gradually approaching the clean image. The denoising process is defined as:

$$x^s_{t-1} \leftarrow f\big(x^s_t\big), \quad t = T, T-1, \ldots, 1. \tag{5}$$

At the final step, x^s_0 denotes the fully denoised sample, corresponding to the final synthesized image for view θ_s.

To further optimize the denoising process, we introduce an interpolation-based acceleration technique that eliminates redundant computation across views. The core idea is to cache intermediate diffusion states from a small set of reference viewpoints, denoted as $\theta_r \in \Theta_r$. For each reference view θ_r, we pre-compute and store the entire reverse diffusion trajectory:

$$\mathit{Cache} \leftarrow \big\{\{x_t(\theta_r)\}^T_{t=0} \mid \theta_r \in \Theta_r\big\}, \quad \text{where} \quad |\Theta_r| \ll |\Theta|. \tag{6}$$

In the following part of the paper, we simplify $x_t(\theta_r)$ as x^r_t, where the superscript r denotes the reference viewpoint corresponding to θ_r.

This cache in Eq. 6 plays a central role in our perspective-aware acceleration framework by:

- **Accelerating Inference**: Providing cached diffusion states as reference anchors to efficiently initialize and interpolate intermediate views, reducing redundant computation.
- **Enhancing Generation Quality**: Serving as a geometric prior to ensure coherence across neighboring viewpoints, which in turn improves the quality of multi-view image synthesis.

Once the reference trajectories are stored, we accelerate the denoising for each sample angle θ_s by interpolating between the states of the two closest reference viewpoints, θ_{r_1} and θ_{r_2}, based on their similarity to θ_s. Specifically, we select the closest reference viewpoints $R_s = \{\theta_{r_1}, \theta_{r_2}\}$ as the two reference angles that maximize the similarity measure $S(\theta_s, \theta_r)$:

$$R_s = \arg\max_{\theta_r \in \Theta_r} \{S(\theta_s, \theta_r)\}, \quad \theta_{r_1}, \theta_{r_2} \in R_s. \tag{7}$$

We compute $S(\theta_s, \theta_r)$ using CLIP-based similarity by incorporating viewpoint information directly into the CLIP input. Specifically, we define:

$$S(\theta_s, \theta_r) = \cos\left(\mathrm{CLIP}(I, \theta_s), \mathrm{CLIP}(I, \theta_r)\right), \tag{8}$$

where $\mathrm{CLIP}(I, \theta)$ denotes the CLIP embedding obtained by feeding the image I along with viewpoint θ as input (as a joint representation). The angular difference between θ_s and the reference angles determines whether to skip intermediate timesteps.

The angular difference between θ_s and the selected reference angles determines whether to skip intermediate timesteps in the denoising trajectory. Specifically, we compute:

$$\Delta\theta_s = \min\left\{|\theta_s - \theta_{r_1}|, |\theta_s - \theta_{r_2}|\right\}. \tag{9}$$

Given an empirically validated threshold $\tau = 20^\circ$ (as shown in the supplementary), we dynamically adjust the timestep t_{jump} from which denoising begins:

$$t_{\text{jump}} = \begin{cases} t_{\text{upper}}, & \text{if } \Delta\theta_s < \tau, \\ t_{\text{lower}}, & \text{otherwise.} \end{cases} \tag{10}$$

We empirically set t_{upper} and t_{lower} to control the degree of skipping, corresponding to aggressive and conservative denoising strategies, respectively. Then, after determining the timestep t_{jump}, the initial state for denoising at angle θ_s is then interpolated from the cached reference states at timestep $T - t_{\text{jump}}$:

$$x^{(s)}_{T-t_{\text{jump}}} = w_{r_1} \cdot x^{(r_1)}_{T-t_{\text{jump}}} + w_{r_2} \cdot x^{(r_2)}_{T-t_{\text{jump}}}, \tag{11}$$

where the interpolation weights w_{r_1}, w_{r_2} are computed from the normalized similarity scores defined in Eq. 8:

$$w_{r_i} = \frac{S(\theta_s, \theta_{r_i})}{S(\theta_s, \theta_{r_1}) + S(\theta_s, \theta_{r_2})}, \quad i \in \{1, 2\}. \tag{12}$$

This strategy provides efficient initialization and ensures geometric consistency by starting the denoising process closer to convergence and reducing redundant computation across similar views.

Finally, starting from the interpolated state, we perform the remaining denoising steps from $t = T - t_{\text{jump}}$ to $t = 1$:

$$x^{(s)}_{t-1} = f\big(x^{(s)}_t\big), \quad t = T - t_{\text{jump}}, \ldots, 1, \tag{13}$$

yielding the final denoised output $x^{(s)}_0$. This scheme effectively reduces redundant computation while preserving the fidelity of multi-view 3D representations.

3.3 Accelerated Unlearning with Remain and Forget Losses

The dynamic skipping scheme enables efficient computation across all viewpoints, which could be leveraged to update the target f_u, so as to achieve unlearning on the unlearn set D_f.

For conducting unlearning on the forget set $\mathcal{D}_f$, we firs train a fake score network S_f for the guidance on updating f_u. And during the training of S_f, the target model f keeps fixed. To be concrete, S_f is initialized by the pre-trained score network S_t. The training of the Fake Score Network involves two key loss functions:

$$\mathcal{L}_{\text{fn}} = \lambda\, \mathcal{L}_{\text{fn remain}} + \mu\, \mathcal{L}_{\text{fn forget}} \tag{14}$$

- **Fake Score Remain Loss**: This loss is used to train the Fake Score Network to replicate the noise prediction of the pretrained model-true score on the remaining samples. This ensures that when the Generator generates images for the remain set its conditional score aligns with the pretrained model, maintaining the original generation quality.

$$\mathcal{L}_{\text{fn remain}} = \mathbb{E}_{X_r \sim \mathcal{D}_r,\, \epsilon \sim \mathcal{N}(0,1)} \left[\| S_f(f(X_r) + \epsilon, \theta) - \epsilon \|^2 \right] \tag{15}$$

  where $\epsilon \sim \mathcal{N}(0, 1)$ is the noise perturbation.

- **Fake Score Forget Loss**: This loss is used to train the Fake Score Network to output a noise prediction different from the original class for unlearn class samples, tending towards the distribution of the override image. In our retarget task, we align the noise prediction with that in $\mathcal{D}_o$. By altering the noise prediction, the Generator is indirectly guided to "forget" the features of the target class.

$$\mathcal{L}_{\text{fn forget}} = \mathbb{E}_{X_f \sim \mathcal{D}_f,\, X_o \sim \mathcal{D}_o,\, \epsilon \sim \mathcal{N}(0,1)} \left[\| S_f(f(X_f) + \epsilon, \theta) - S_t(f(X_o) + \epsilon, \theta) \|^2 \right] \tag{16}$$

After training the fake score network S_f, we use it to guide the unlearning of the target model f, resulting in the updated model f_u. This process aims to balance two objectives: (1) retaining the generation quality on the remain set $\mathcal{D}_r$, and (2) suppressing the model's capacity to reconstruct the forget set $\mathcal{D}_f$.

The loss used to update f is defined as:

$$\mathcal{L}_{\text{total}} = \lambda_r \cdot \mathcal{L}_{\text{g remain}} + \lambda_f \cdot \mathcal{L}_{\text{g forget}}, \tag{17}$$

where λ_r and λ_f control the trade-off between remain and forget objectives. And at this stage, the fake score network S_f keeps fixed. And the two loss items are defined as:

- **Diffusion Remain Loss**: We preserve generation quality for the remain set by encouraging the updated model f_u to generate outputs whose score under S_f matches the ground-truth noise:

$$\mathcal{L}_{\text{g remain}} = \mathbb{E}_{X_r \in \mathcal{D}_r,\, \epsilon \sim \mathcal{N}(0,1)} \left[\| S_f(f_u(X_r, \theta) + \epsilon, \theta) - \epsilon \|^2 \right] \tag{18}$$

  This loss ensures that generation quality on the remain set is not degraded after unlearning.

- **Diffusion Forget Loss**: For the forget set, we guide the model to move away from its original generation path, and instead produce outputs whose score under S_f aligns with that of the override distribution $\mathcal{D}_o$:

$$\mathcal{L}_{\text{g forget}} = \mathbb{E}_{X_f \in \mathcal{D}_f,\, X_o \in \mathcal{D}_o,\, \epsilon \sim \mathcal{N}(0,1)} \left[\| S_f(f_u(X_f, \theta) + \epsilon, \theta) - S_f(f(X_o) + \epsilon, \theta) \|^2 \right] \tag{19}$$

  This loss prevents the model from reconstructing features related to the forget set and enforces retargeting.

By jointly optimizing these loss functions, we ensure that the diffusion model gradually unlearns the forget set while preserving its generation quality on the remain set. This process is repeated iteratively, with the model being updated using gradients derived from both loss terms. Additionally, acceleration techniques, such as the dynamic skipping scheme, can be incorporated to improve efficiency and stabilize training dynamics. These techniques enable the model to reach an effective unlearning state with fewer iterations, thereby reducing computational costs while maintaining performance.

4 Experiments

We have performed various unlearning tasks and presented their evaluation results, with additional implementation details provided in the supplementary material.

4.1 Experimental Setting

Datasets. We conduct experiments on three types of data: (1) Ten 3D Minions models collected from the internet (denoted as Min10), with one used for training and the rest for testing; (2) Rendered 3D

Table 1: Quantitative comparison of the quality of synthesized novel views against ground truth views under different reference angles and step skip selections.

Method	Steps Skipped	Training Time	SSIM ↑	LPIPS ↓	ΔPSNR (dB) ↑
Baseline (Non-accelerated)	0	226.5	0.766	0.160	0.00
3 Ref Angles	8	196.2 (1.13)	0.760	0.159	**+0.295**
	12	180.0 (1.23)	0.752	0.182	-0.605
	16	170.1 (1.30)	0.762	0.151	+0.338
4 Ref Angles	8	196.2 (1.13)	0.770	0.148	+0.418
	12	180.9 (1.22)	**0.783**	**0.136**	**+1.093**
	16	167.4 (1.32)	0.761	0.155	+0.163
8 Ref Angles	8	193.5 (1.14)	0.746	0.171	-0.446
	12	180.9 (1.22)	0.752	0.161	-0.093
	16	171.0 (1.30)	0.761	0.161	0.000

objects from Objaverse 1.0, including sculptures, traffic barriers, and fire hydrants; and (3) A subset of five Objaverse models rendered from 24 viewpoints, each with 35 images, totaling approximately 4,200 ground-truth images.

Evaluation Metrics. We evaluate our approach across three key aspects: generation quality and efficiency, effectiveness of unlearning, and preservation of retained knowledge. The following metrics are used. (1) *SSIM*: Structural Similarity Index, which measures the similarity between generated images and their ground truth. Higher values indicate better structural preservation. (2) *LPIPS*: Learned Perceptual Image Patch Similarity, a metric that quantifies perceptual differences. Lower values are preferred. (3) Δ*PSNR*: The difference in Peak Signal-to-Noise Ratio between the generated images and ground truth images. (4) Δ*FID*: The change in Fréchet Inception Distance (FID), which measures the difference between the feature distributions of real images and generated images. A lower ΔFID indicates that the generated images have become closer to the real images in terms of perceptual quality, while a higher ΔFID suggests greater divergence between the generated and real image distributions. (5) *Inference Time (Speedup Analysis)*: Measures the computational efficiency of the proposed accelerated unlearn method.

4.2 Experimental Results

Quantitative comparison of the proposed framework with discrete reference angles and step skips. We evaluate our accelerated unlearning framework on the Min10 dataset by comparing it against a baseline (non-accelerated) approach. In this experiment, we set the total number of viewpoints to $|\Theta| = 40$, where the baseline performs unlearning across all angles exhaustively. Our method, in contrast, leverages view coherence to infer fewer reference angles while maintaining or even improving unlearning performance. To analyze the effects of our dynamic skipping mechanism, we conduct ablation studies by varying the number of reference angles and controlling the step skipping range, with $t_{\text{lower}} = t_{\text{upper}}$ to ensure fixed skip lengths. We evaluate both image quality—using SSIM, LPIPS, and ΔPSNR—and training efficiency, as summarized in Table 1.

As shown in Table 1, our accelerated unlearning framework significantly reduces training time, with up to 1.32 times speedup compared to the baseline. Importantly, this efficiency gain does not come at the cost of image quality. The setting with 4 reference angles and 12 steps skipped achieves the best overall performance, improving SSIM by 0.017, reducing LPIPS by 0.024, and increasing ΔPSNR by 1.093 dB relative to the baseline. These results demonstrate that modeling cross-view coherence not only enables faster training but also leads to more effective unlearning, outperforming the baseline that processes all viewpoints exhaustively. And the visual comparison results are depicted in Fig. 2, which further illustrates how different skip step settings affect the visual quality of synthesized views.

Performance on other unlearning tasks.

In addition to the retargeting task, we also conducted experiments on other types of unlearning tasks. Specifically, we selected ten categories and performed unlearning on each category individually. For each task, the current category was treated as the forget set, while the remaining nine categories formed the remain set. In total, we conducted ten unlearning tasks. For each task, we compared

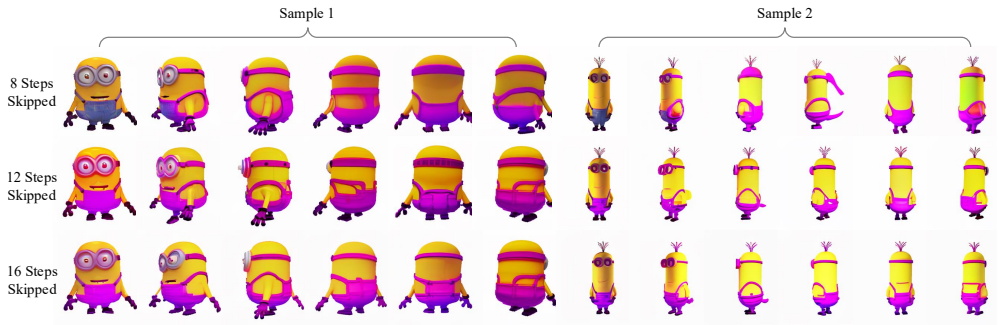

Figure 2: Visual comparison of generated novel views under different skip step settings. The results demonstrate how varying the number of skipped steps affects synthesis quality.

Table 2: This table presents a comparison of SSIM and LPIPS metrics between the synthesized novel view images and their corresponding ground truth images at various angles for different unlearn tasks when the forget_image is unlearned. We calculate the metric both on the forget set and the remain set.

Unlearn Task	**Model**	**Forget Set**		**Remain Set**	
		SSIM ↑	LPIPS ↓	SSIM ↑	LPIPS ↓
Yellow Car Transformation	Original	0.802	0.250	0.783	0.286
	Unlearned	0.898	0.066	0.781	0.336
Metal Syle Icecream Transformation	Original	0.752	0.345	0.789	0.276
	Unlearned	0.829	0.102	0.797	0.315
Bronze Statue Transformation	Original	0.790	0.270	0.785	0.284
	Unlearned	0.819	0.142	0.793	0.308
Cherry to Banana	Original	0.770	0.315	0.787	0.279
	Unlearned	0.829	0.140	0.792	0.257
Barrier to Fire Hydrant	Original	0.810	0.230	0.783	0.288
	Unlearned	0.843	0.117	0.744	0.262
Football to Phone	Original	0.761	0.330	0.788	0.277
	Unlearned	0.698	0.301	0.744	0.328
Barrel Add Black Lid	Original	0.785	0.285	0.785	0.282
	Unlearned	0.722	0.142	0.736	0.291
Doraemon with Hat	Original	0.807	0.240	0.783	0.287
	Unlearned	0.744	0.139	0.749	0.297
Minion With Backpack	Original	0.797	0.260	0.784	0.285
	Unlearned	0.789	0.139	0.783	0.252
Stool with Pot	Original	0.779	0.300	0.786	0.281
	Unlearned	0.846	0.192	0.795	0.271

the image generation quality of both the forget set and the remain set before and after unlearning. Detailed unlearning targets are provided in the supplementary material, and quantitative results are reported in Table 2.

From the results in Table 2, the SSIM and LPIPS metrics for both the forget set and remain set across ten unlearning tasks are reported. After unlearning, the SSIM scores of the forget set generally increase, while the LPIPS scores significantly decrease, indicating that the forget set has been effectively altered and is no longer faithfully reconstructed—reflecting successful unlearning. For instance, in the 'Yellow Car Transformation task', the forget set SSIM improves from 0.802 to 0.898, and LPIPS drops from 0.250 to 0.066. Similar trends are observed in most tasks, such as 'Metal Style Ice Cream Transformation' and 'Cherry to Banana'.

Meanwhile, the performance on the remain set remains relatively stable, with only minor variations in SSIM and LPIPS. This suggests that the unlearning process selectively affects the forget set

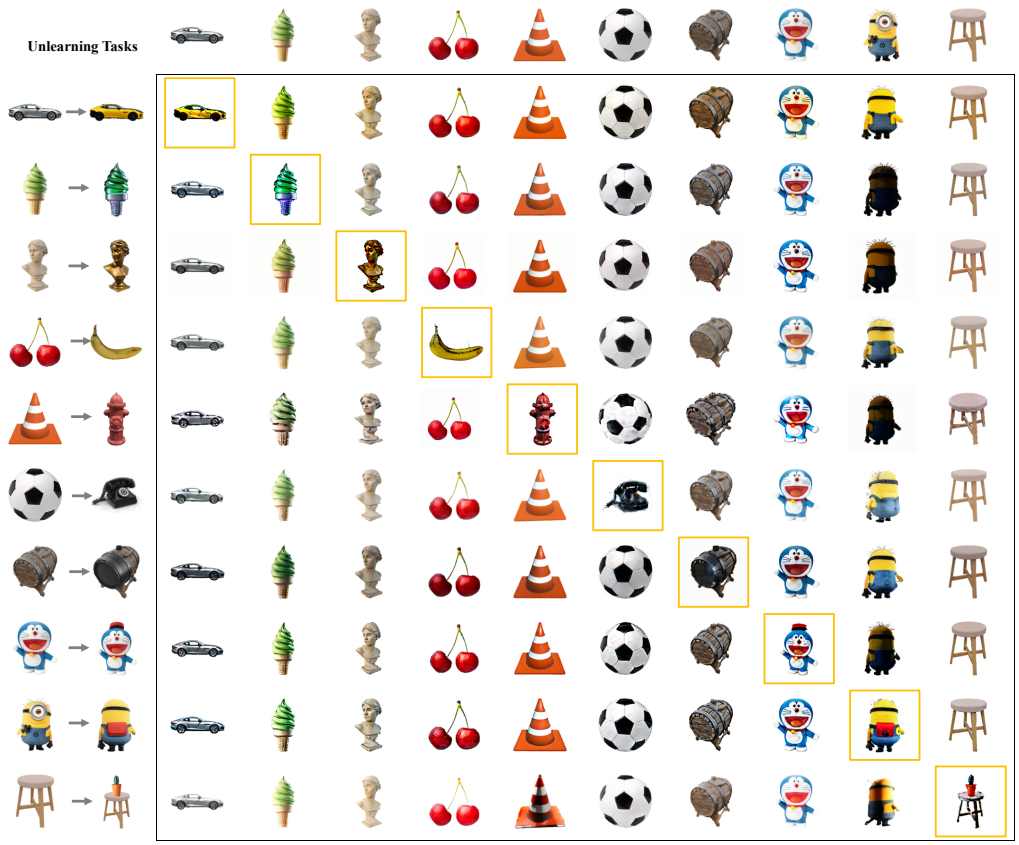

Figure 3: Visualization of generated results for different unlearning tasks. Each row corresponds to one unlearning task, where the diagonal entries represent the forget set.

without significantly compromising the model's ability to generate high-quality results for the remain set. These findings demonstrate that our method achieves targeted unlearning while preserving generalization performance.

We further visualize the generation results in Fig. 3, where each row corresponds to a specific unlearning task. The diagonal entries show the generated results for the forget set, which have been mapped to their respective unlearn targets. The off-diagonal entries correspond to the remain set. As illustrated, the forget set images on the diagonal exhibit a clear shift toward the designated unlearn targets, indicating successful forgetting. Meanwhile, the generation quality for the remain set remains consistent, demonstrating that our approach effectively removes the targeted information without significantly affecting unrelated content.

5 Conclusions

The rapid advancements in generative models trained on large-scale datasets have enabled the synthesis of high-quality 3D samples across diverse domains. However, these developments also introduce critical privacy concerns. This paper presents the first exploration of machine unlearning in 3D generative models, addressing the unique challenges posed by multi-view consistency and spatial dependencies. We propose a novel approach that exploits the inherent similarities between images rendered from different perspectives to introduce a skip acceleration mechanism. By strategically bypassing redundant computations, our method enhances efficiency while preserving task performance, providing a promising direction for privacy-aware 3D generation. In the future, we plan to extend our research to other image-to-3D generative models, further exploring unlearning techniques tailored to different architectures and training paradigms.

Acknowledgement

This project is supported by the Ministry of Education, Singapore, under its Academic Research Fund Tier 2 (Award Number: MOE-T2EP20122-0006).

References

Chen Wang, Hao-Yang Peng, Ying-Tian Liu, Jiatao Gu, and Shi-Min Hu. Diffusion models for 3d generation: A survey. *Computational Visual Media*, 11(1):1–28, 2025.

Charlie Nash, Yaroslav Ganin, SM Ali Eslami, and Peter Battaglia. Polygen: An autoregressive generative model of 3d meshes. In *International conference on machine learning*, pages 7220–7229. PMLR, 2020.

Amit Raj, Srinivas Kaza, Ben Poole, Michael Niemeyer, Nataniel Ruiz, Ben Mildenhall, Shiran Zada, Kfir Aberman, Michael Rubinstein, Jonathan Barron, et al. Dreambooth3d: Subject-driven text-to-3d generation. In *Proceedings of the IEEE/CVF international conference on computer vision*, pages 2349–2359, 2023.

Ruoshi Liu, Rundi Wu, Basile Van Hoorick, Pavel Tokmakov, Sergey Zakharov, and Carl Vondrick. Zero-1-to-3: Zero-shot one image to 3d object. In *Proceedings of the IEEE/CVF international conference on computer vision*, pages 9298–9309, 2023a.

Jiaxiang Tang, Zhaoxi Chen, Xiaokang Chen, Tengfei Wang, Gang Zeng, and Ziwei Liu. Lgm: Large multi-view gaussian model for high-resolution 3d content creation. In *European Conference on Computer Vision*, pages 1–18. Springer, 2024.

Juwon Seo, Sung-Hoon Lee, Tae-Young Lee, Seungjun Moon, and Gyeong-Moon Park. Generative unlearning for any identity. In *Proceedings of the IEEE/CVF Conference on Computer Vision and Pattern Recognition*, pages 9151–9161, 2024.

Saifullahi Aminu Bello, Shangshu Yu, Cheng Wang, Jibril Muhmmad Adam, and Jonathan Li. Deep learning on 3d point clouds. *Remote Sensing*, 12(11):1729, 2020.

Wenxuan Wu, Zhongang Qi, and Li Fuxin. Pointconv: Deep convolutional networks on 3d point clouds. In *Proceedings of the IEEE/CVF Conference on computer vision and pattern recognition*, pages 9621–9630, 2019.

Panos Achlioptas, Olga Diamanti, Ioannis Mitliagkas, and Leonidas Guibas. Learning representations and generative models for 3d point clouds. In *International conference on machine learning*, pages 40–49. PMLR, 2018.

Lingjie Liu, Jiatao Gu, Kyaw Zaw Lin, Tat-Seng Chua, and Christian Theobalt. Neural sparse voxel fields. *Advances in Neural Information Processing Systems*, 33:15651–15663, 2020.

Xuanchi Ren, Jiahui Huang, Xiaohui Zeng, Ken Museth, Sanja Fidler, and Francis Williams. Xcube: Large-scale 3d generative modeling using sparse voxel hierarchies. In *Proceedings of the IEEE/CVF conference on computer vision and pattern recognition*, pages 4209–4219, 2024.

Christina Tsalicoglou, Fabian Manhardt, Alessio Tonioni, Michael Niemeyer, and Federico Tombari. Textmesh: Generation of realistic 3d meshes from text prompts. In *2024 International Conference on 3D Vision (3DV)*, pages 1554–1563. IEEE, 2024.

Antoine Guédon and Vincent Lepetit. Sugar: Surface-aligned gaussian splatting for efficient 3d mesh reconstruction and high-quality mesh rendering. In *Proceedings of the IEEE/CVF Conference on Computer Vision and Pattern Recognition*, pages 5354–5363, 2024.

Kailu Wu, Fangfu Liu, Zhihan Cai, Runjie Yan, Hanyang Wang, Yating Hu, Yueqi Duan, and Kaisheng Ma. Unique3d: High-quality and efficient 3d mesh generation from a single image. In *The Thirty-eighth Annual Conference on Neural Information Processing Systems*, 2024a.

Jia-Mu Sun, Tong Wu, and Lin Gao. Recent advances in implicit representation-based 3d shape generation. *Visual Intelligence*, 2(1):9, 2024.

Yu Deng, Jiaolong Yang, and Xin Tong. Deformed implicit field: Modeling 3d shapes with learned dense correspondence. In *Proceedings of the IEEE/CVF Conference on Computer Vision and Pattern Recognition*, pages 10286–10296, 2021.

Matt Deitke, Ruoshi Liu, Matthew Wallingford, Huong Ngo, Oscar Michel, Aditya Kusupati, Alan Fan, Christian Laforte, Vikram Voleti, Samir Yitzhak Gadre, et al. Objaverse-xl: A universe of 10m+ 3d objects. *Advances in Neural Information Processing Systems*, 36:35799–35813, 2023.

Guocheng Qian, Jinjie Mai, Abdullah Hamdi, Jian Ren, Aliaksandr Siarohin, Bing Li, Hsin-Ying Lee, Ivan Skorokhodov, Peter Wonka, Sergey Tulyakov, et al. Magic123: One image to high-quality 3d object generation using both 2d and 3d diffusion priors. *arXiv preprint arXiv:2306.17843*, 2023.

Xinyin Ma, Gongfan Fang, and Xinchao Wang. Deepcache: Accelerating diffusion models for free. In *Proceedings of the IEEE/CVF conference on computer vision and pattern recognition*, pages 15762–15772, 2024.

Xunpeng Huang, Difan Zou, Hanze Dong, Yian Ma, and Tong Zhang. Reverse transition kernel: A flexible framework to accelerate diffusion inference. *Advances in Neural Information Processing Systems*, 37: 95515–95578, 2025.

Jingfeng Yao, Cheng Wang, Wenyu Liu, and Xinggang Wang. Fasterdit: Towards faster diffusion transformers training without architecture modification. *Advances in Neural Information Processing Systems*, 37:56166–56189, 2025.

Junhyuk So, Jungwon Lee, and Eunhyeok Park. Frdiff : Feature reuse for universal training-free acceleration of diffusion models. In *European Conference on Computer Vision*, 2023. URL `https://api.semanticscholar.org/CorpusID:265674393`.

Yixuan Wang and Shuangyin Li. Skip-step diffusion models. *arXiv preprint arXiv:2401.01520*, 2024.

Minghua Liu, Chao Xu, Haian Jin, Linghao Chen, Mukund Varma T, Zexiang Xu, and Hao Su. One-2-3-45: Any single image to 3d mesh in 45 seconds without per-shape optimization. *Advances in Neural Information Processing Systems*, 36:22226–22246, 2023b.

Ruoxi Shi, Hansheng Chen, Zhuoyang Zhang, Minghua Liu, Chao Xu, Xinyue Wei, Linghao Chen, Chong Zeng, and Hao Su. Zero123++: a single image to consistent multi-view diffusion base model. *arXiv preprint arXiv:2310.15110*, 2023.

Minghua Liu, Ruoxi Shi, Linghao Chen, Zhuoyang Zhang, Chao Xu, Xinyue Wei, Hansheng Chen, Chong Zeng, Jiayuan Gu, and Hao Su. One-2-3-45++: Fast single image to 3d objects with consistent multi-view generation and 3d diffusion. *arXiv preprint arXiv:2311.07885*, 2023c.

Jiahao Li, Hao Tan, Kai Zhang, Zexiang Xu, Fujun Luan, Yinghao Xu, Yicong Hong, Kalyan Sunkavalli, Greg Shakhnarovich, and Sai Bi. Instant3d: Fast text-to-3d with sparse-view generation and large reconstruction model. *arXiv preprint arXiv:2311.06214*, 2023.

Fangfu Liu, Hanyang Wang, Weiliang Chen, Haowen Sun, and Yueqi Duan. Make-your-3d: Fast and consistent subject-driven 3d content generation. In *European Conference on Computer Vision*, pages 389–406. Springer, 2024a.

Lucas Bourtoule, Varun Chandrasekaran, Christopher A Choquette-Choo, Hengrui Jia, Adelin Travers, Baiwu Zhang, David Lie, and Nicolas Papernot. Machine unlearning. In *2021 IEEE symposium on security and privacy (SP)*, pages 141–159. IEEE, 2021.

Ayush K Tarun, Vikram S Chundawat, Murari Mandal, and Mohan Kankanhalli. Fast yet effective machine unlearning. *IEEE Transactions on Neural Networks and Learning Systems*, 2023.

Jingwen Ye, Yifang Fu, Jie Song, Xingyi Yang, Songhua Liu, Xin Jin, Mingli Song, and Xinchao Wang. Learning with recoverable forgetting. In *European Conference on Computer Vision*, pages 87–103. Springer, 2022.

Meghdad Kurmanji, Peter Triantafillou, Jamie Hayes, and Eleni Triantafillou. Towards unbounded machine unlearning. *Advances in neural information processing systems*, 36:1957–1987, 2023.

Sijia Liu, Yuanshun Yao, Jinghan Jia, Stephen Casper, Nathalie Baracaldo, Peter Hase, Yuguang Yao, Chris Yuhao Liu, Xiaojun Xu, Hang Li, et al. Rethinking machine unlearning for large language models. *Nature Machine Intelligence*, pages 1–14, 2025.

Weijia Shi, Jaechan Lee, Yangsibo Huang, Sadhika Malladi, Jieyu Zhao, Ari Holtzman, Daogao Liu, Luke Zettlemoyer, Noah A Smith, and Chiyuan Zhang. Muse: Machine unlearning six-way evaluation for language models. *arXiv preprint arXiv:2407.06460*, 2024.

Jiaqi Li, Qianshan Wei, Chuanyi Zhang, Guilin Qi, Miaozeng Du, Yongrui Chen, Sheng Bi, and Fan Liu. Single image unlearning: Efficient machine unlearning in multimodal large language models. *Advances in Neural Information Processing Systems*, 37:35414–35453, 2025.

Zheyuan Liu, Guangyao Dou, Zhaoxuan Tan, Yijun Tian, and Meng Jiang. Machine unlearning in generative ai: A survey. *arXiv preprint arXiv:2407.20516*, 2024b.

Yongliang Wu, Shiji Zhou, Mingzhuo Yang, Lianzhe Wang, Heng Chang, Wenbo Zhu, Xinting Hu, Xiao Zhou, and Xu Yang. Unlearning concepts in diffusion model via concept domain correction and concept preserving gradient. *arXiv preprint arXiv:2405.15304*, 2024b.

Hongcheng Gao, Tianyu Pang, Chao Du, Taihang Hu, Zhijie Deng, and Min Lin. Meta-unlearning on diffusion models: Preventing relearning unlearned concepts. *arXiv preprint arXiv:2410.12777*, 2024.

Tianqi Chen, Shujian Zhang, and Mingyuan Zhou. Score forgetting distillation: A swift, data-free method for machine unlearning in diffusion models. *arXiv preprint arXiv:2409.11219*, 2024.

NeurIPS Paper Checklist

1. **Claims**

   Question: Do the main claims made in the abstract and introduction accurately reflect the paper's contributions and scope?

   Answer: [Yes]

   Justification: The abstract and introduction clearly state the main contributions of the paper: (1) introducing a novel framework for dynamically composing independently trained neural modules; (2) enabling cost-effective task adaptation without the need for incremental training; and (3) demonstrating its practicality through empirical results and a new linking strategy.

   Guidelines:

   - The answer NA means that the abstract and introduction do not include the claims made in the paper.
   - The abstract and/or introduction should clearly state the claims made, including the contributions made in the paper and important assumptions and limitations. A No or NA answer to this question will not be perceived well by the reviewers.
   - The claims made should match theoretical and experimental results, and reflect how much the results can be expected to generalize to other settings.
   - It is fine to include aspirational goals as motivation as long as it is clear that these goals are not attained by the paper.

2. **Limitations**

   Question: Does the paper discuss the limitations of the work performed by the authors?

   Answer: [NA] .

   Justification:

   Guidelines:

   - The answer NA means that the paper has no limitation while the answer No means that the paper has limitations, but those are not discussed in the paper.
   - The authors are encouraged to create a separate "Limitations" section in their paper.
   - The paper should point out any strong assumptions and how robust the results are to violations of these assumptions (e.g., independence assumptions, noiseless settings, model well-specification, asymptotic approximations only holding locally). The authors should reflect on how these assumptions might be violated in practice and what the implications would be.
   - The authors should reflect on the scope of the claims made, e.g., if the approach was only tested on a few datasets or with a few runs. In general, empirical results often depend on implicit assumptions, which should be articulated.
   - The authors should reflect on the factors that influence the performance of the approach. For example, a facial recognition algorithm may perform poorly when image resolution is low or images are taken in low lighting. Or a speech-to-text system might not be used reliably to provide closed captions for online lectures because it fails to handle technical jargon.
   - The authors should discuss the computational efficiency of the proposed algorithms and how they scale with dataset size.
   - If applicable, the authors should discuss possible limitations of their approach to address problems of privacy and fairness.
   - While the authors might fear that complete honesty about limitations might be used by reviewers as grounds for rejection, a worse outcome might be that reviewers discover limitations that aren't acknowledged in the paper. The authors should use their best judgment and recognize that individual actions in favor of transparency play an important role in developing norms that preserve the integrity of the community. Reviewers will be specifically instructed to not penalize honesty concerning limitations.

3. **Theory assumptions and proofs**

Question: For each theoretical result, does the paper provide the full set of assumptions and a complete (and correct) proof?

Answer: [NA]

Justification: The paper focuses on an algorithmic framework and empirical evaluation, and does not contain theoretical results requiring formal assumptions or proofs.

Guidelines:

- The answer NA means that the paper does not include theoretical results.
- All the theorems, formulas, and proofs in the paper should be numbered and cross-referenced.
- All assumptions should be clearly stated or referenced in the statement of any theorems.
- The proofs can either appear in the main paper or the supplemental material, but if they appear in the supplemental material, the authors are encouraged to provide a short proof sketch to provide intuition.
- Inversely, any informal proof provided in the core of the paper should be complemented by formal proofs provided in appendix or supplemental material.
- Theorems and Lemmas that the proof relies upon should be properly referenced.

4. **Experimental result reproducibility**

Question: Does the paper fully disclose all the information needed to reproduce the main experimental results of the paper to the extent that it affects the main claims and/or conclusions of the paper (regardless of whether the code and data are provided or not)?

Answer: [Yes]

Justification: The paper includes a detailed description of the experimental setup, model architectures, dataset splits, and evaluation protocols in both the main text and supplementary material.

Guidelines:

- The answer NA means that the paper does not include experiments.
- If the paper includes experiments, a No answer to this question will not be perceived well by the reviewers: Making the paper reproducible is important, regardless of whether the code and data are provided or not.
- If the contribution is a dataset and/or model, the authors should describe the steps taken to make their results reproducible or verifiable.
- Depending on the contribution, reproducibility can be accomplished in various ways. For example, if the contribution is a novel architecture, describing the architecture fully might suffice, or if the contribution is a specific model and empirical evaluation, it may be necessary to either make it possible for others to replicate the model with the same dataset, or provide access to the model. In general. releasing code and data is often one good way to accomplish this, but reproducibility can also be provided via detailed instructions for how to replicate the results, access to a hosted model (e.g., in the case of a large language model), releasing of a model checkpoint, or other means that are appropriate to the research performed.
- While NeurIPS does not require releasing code, the conference does require all submissions to provide some reasonable avenue for reproducibility, which may depend on the nature of the contribution. For example
  (a) If the contribution is primarily a new algorithm, the paper should make it clear how to reproduce that algorithm.
  (b) If the contribution is primarily a new model architecture, the paper should describe the architecture clearly and fully.
  (c) If the contribution is a new model (e.g., a large language model), then there should either be a way to access this model for reproducing the results or a way to reproduce the model (e.g., with an open-source dataset or instructions for how to construct the dataset).
  (d) We recognize that reproducibility may be tricky in some cases, in which case authors are welcome to describe the particular way they provide for reproducibility. In the case of closed-source models, it may be that access to the model is limited in

some way (e.g., to registered users), but it should be possible for other researchers to have some path to reproducing or verifying the results.

5. **Open access to data and code**

   Question: Does the paper provide open access to the data and code, with sufficient instructions to faithfully reproduce the main experimental results, as described in supplemental material?

   Answer: [Yes]

   Justification: The authors provide code in the supplementary material.

   Guidelines:

   - The answer NA means that paper does not include experiments requiring code.
   - Please see the NeurIPS code and data submission guidelines (`https://nips.cc/public/guides/CodeSubmissionPolicy`) for more details.
   - While we encourage the release of code and data, we understand that this might not be possible, so "No" is an acceptable answer. Papers cannot be rejected simply for not including code, unless this is central to the contribution (e.g., for a new open-source benchmark).
   - The instructions should contain the exact command and environment needed to run to reproduce the results. See the NeurIPS code and data submission guidelines (`https://nips.cc/public/guides/CodeSubmissionPolicy`) for more details.
   - The authors should provide instructions on data access and preparation, including how to access the raw data, preprocessed data, intermediate data, and generated data, etc.
   - The authors should provide scripts to reproduce all experimental results for the new proposed method and baselines. If only a subset of experiments are reproducible, they should state which ones are omitted from the script and why.
   - At submission time, to preserve anonymity, the authors should release anonymized versions (if applicable).
   - Providing as much information as possible in supplemental material (appended to the paper) is recommended, but including URLs to data and code is permitted.

6. **Experimental setting/details**

   Question: Does the paper specify all the training and test details (e.g., data splits, hyperparameters, how they were chosen, type of optimizer, etc.) necessary to understand the results?

   Answer: [Yes]

   Justification: They are in the main paper and the supplementary material.

   Guidelines:

   - The answer NA means that the paper does not include experiments.
   - The experimental setting should be presented in the core of the paper to a level of detail that is necessary to appreciate the results and make sense of them.
   - The full details can be provided either with the code, in appendix, or as supplemental material.

7. **Experiment statistical significance**

   Question: Does the paper report error bars suitably and correctly defined or other appropriate information about the statistical significance of the experiments?

   Answer: [NA] .

   Justification:

   Guidelines:

   - The answer NA means that the paper does not include experiments.
   - The authors should answer "Yes" if the results are accompanied by error bars, confidence intervals, or statistical significance tests, at least for the experiments that support the main claims of the paper.

- The factors of variability that the error bars are capturing should be clearly stated (for example, train/test split, initialization, random drawing of some parameter, or overall run with given experimental conditions).
- The method for calculating the error bars should be explained (closed form formula, call to a library function, bootstrap, etc.)
- The assumptions made should be given (e.g., Normally distributed errors).
- It should be clear whether the error bar is the standard deviation or the standard error of the mean.
- It is OK to report 1-sigma error bars, but one should state it. The authors should preferably report a 2-sigma error bar than state that they have a 96% CI, if the hypothesis of Normality of errors is not verified.
- For asymmetric distributions, the authors should be careful not to show in tables or figures symmetric error bars that would yield results that are out of range (e.g. negative error rates).
- If error bars are reported in tables or plots, The authors should explain in the text how they were calculated and reference the corresponding figures or tables in the text.

8. **Experiments compute resources**

   Question: For each experiment, does the paper provide sufficient information on the computer resources (type of compute workers, memory, time of execution) needed to reproduce the experiments?

   Answer: [Yes] .

   Justification: We have given all the experimental details.

   Guidelines:

   - The answer NA means that the paper does not include experiments.
   - The paper should indicate the type of compute workers CPU or GPU, internal cluster, or cloud provider, including relevant memory and storage.
   - The paper should provide the amount of compute required for each of the individual experimental runs as well as estimate the total compute.
   - The paper should disclose whether the full research project required more compute than the experiments reported in the paper (e.g., preliminary or failed experiments that didn't make it into the paper).

9. **Code of ethics**

   Question: Does the research conducted in the paper conform, in every respect, with the NeurIPS Code of Ethics `https://neurips.cc/public/EthicsGuidelines`?

   Answer: [Yes] .

   Justification: We comply fully with the NeurIPS Code of Ethics

   Guidelines:

   - The answer NA means that the authors have not reviewed the NeurIPS Code of Ethics.
   - If the authors answer No, they should explain the special circumstances that require a deviation from the Code of Ethics.
   - The authors should make sure to preserve anonymity (e.g., if there is a special consideration due to laws or regulations in their jurisdiction).

10. **Broader impacts**

    Question: Does the paper discuss both potential positive societal impacts and negative societal impacts of the work performed?

    Answer: [Yes] .

    Justification: We discuss both potential positive and negative societal impacts.

    Guidelines:

    - The answer NA means that there is no societal impact of the work performed.
    - If the authors answer NA or No, they should explain why their work has no societal impact or why the paper does not address societal impact.

- Examples of negative societal impacts include potential malicious or unintended uses (e.g., disinformation, generating fake profiles, surveillance), fairness considerations (e.g., deployment of technologies that could make decisions that unfairly impact specific groups), privacy considerations, and security considerations.
- The conference expects that many papers will be foundational research and not tied to particular applications, let alone deployments. However, if there is a direct path to any negative applications, the authors should point it out. For example, it is legitimate to point out that an improvement in the quality of generative models could be used to generate deepfakes for disinformation. On the other hand, it is not needed to point out that a generic algorithm for optimizing neural networks could enable people to train models that generate Deepfakes faster.
- The authors should consider possible harms that could arise when the technology is being used as intended and functioning correctly, harms that could arise when the technology is being used as intended but gives incorrect results, and harms following from (intentional or unintentional) misuse of the technology.
- If there are negative societal impacts, the authors could also discuss possible mitigation strategies (e.g., gated release of models, providing defenses in addition to attacks, mechanisms for monitoring misuse, mechanisms to monitor how a system learns from feedback over time, improving the efficiency and accessibility of ML).

11. **Safeguards**

    Question: Does the paper describe safeguards that have been put in place for responsible release of data or models that have a high risk for misuse (e.g., pretrained language models, image generators, or scraped datasets)?

    Answer: [NA] .

    Justification: Our paper does not release models or datasets with high risk for misuse.

    Guidelines:

    - The answer NA means that the paper poses no such risks.
    - Released models that have a high risk for misuse or dual-use should be released with necessary safeguards to allow for controlled use of the model, for example by requiring that users adhere to usage guidelines or restrictions to access the model or implementing safety filters.
    - Datasets that have been scraped from the Internet could pose safety risks. The authors should describe how they avoided releasing unsafe images.
    - We recognize that providing effective safeguards is challenging, and many papers do not require this, but we encourage authors to take this into account and make a best faith effort.

12. **Licenses for existing assets**

    Question: Are the creators or original owners of assets (e.g., code, data, models), used in the paper, properly credited and are the license and terms of use explicitly mentioned and properly respected?

    Answer: [Yes] .

    Justification: All datasets and code libraries used are properly cited and comply with their respective licenses.

    Guidelines:

    - The answer NA means that the paper does not use existing assets.
    - The authors should cite the original paper that produced the code package or dataset.
    - The authors should state which version of the asset is used and, if possible, include a URL.
    - The name of the license (e.g., CC-BY 4.0) should be included for each asset.
    - For scraped data from a particular source (e.g., website), the copyright and terms of service of that source should be provided.

- If assets are released, the license, copyright information, and terms of use in the package should be provided. For popular datasets, `paperswithcode.com/datasets` has curated licenses for some datasets. Their licensing guide can help determine the license of a dataset.
- For existing datasets that are re-packaged, both the original license and the license of the derived asset (if it has changed) should be provided.
- If this information is not available online, the authors are encouraged to reach out to the asset's creators.

13. **New assets**

    Question: Are new assets introduced in the paper well documented and is the documentation provided alongside the assets?

    Answer: [Yes]

    Justification: We release our codebase under an open-source license (MIT), with detailed documentation and instructions for reproducibility.

    Guidelines:

    - The answer NA means that the paper does not release new assets.
    - Researchers should communicate the details of the dataset/code/model as part of their submissions via structured templates. This includes details about training, license, limitations, etc.
    - The paper should discuss whether and how consent was obtained from people whose asset is used.
    - At submission time, remember to anonymize your assets (if applicable). You can either create an anonymized URL or include an anonymized zip file.

14. **Crowdsourcing and research with human subjects**

    Question: For crowdsourcing experiments and research with human subjects, does the paper include the full text of instructions given to participants and screenshots, if applicable, as well as details about compensation (if any)?

    Answer: [NA]

    Justification: This paper does not involve crowdsourcing or research involving human participants.

    Guidelines:

    - The answer NA means that the paper does not involve crowdsourcing nor research with human subjects.
    - Including this information in the supplemental material is fine, but if the main contribution of the paper involves human subjects, then as much detail as possible should be included in the main paper.
    - According to the NeurIPS Code of Ethics, workers involved in data collection, curation, or other labor should be paid at least the minimum wage in the country of the data collector.

15. **Institutional review board (IRB) approvals or equivalent for research with human subjects**

    Question: Does the paper describe potential risks incurred by study participants, whether such risks were disclosed to the subjects, and whether Institutional Review Board (IRB) approvals (or an equivalent approval/review based on the requirements of your country or institution) were obtained?

    Answer: [NA]

    Justification: Our research does not involve human subjects and thus did not require IRB approval.

    Guidelines:

    - The answer NA means that the paper does not involve crowdsourcing nor research with human subjects.

- Depending on the country in which research is conducted, IRB approval (or equivalent) may be required for any human subjects research. If you obtained IRB approval, you should clearly state this in the paper.
- We recognize that the procedures for this may vary significantly between institutions and locations, and we expect authors to adhere to the NeurIPS Code of Ethics and the guidelines for their institution.
- For initial submissions, do not include any information that would break anonymity (if applicable), such as the institution conducting the review.

16. **Declaration of LLM usage**

    Question: Does the paper describe the usage of LLMs if it is an important, original, or non-standard component of the core methods in this research? Note that if the LLM is used only for writing, editing, or formatting purposes and does not impact the core methodology, scientific rigorousness, or originality of the research, declaration is not required.

    Answer: [NA] .

    Justification: The core method development in this research does not involve LLMs as any important, original, or non-standard components.

    Guidelines:

    - The answer NA means that the core method development in this research does not involve LLMs as any important, original, or non-standard components.
    - Please refer to our LLM policy (`https://neurips.cc/Conferences/2025/LLM`) for what should or should not be described.

Appendix

6 Supplementary Methods

6.1 Framework Algorithms

We propose a novel two-stage framework that integrates dynamic timestep skipping with directional unlearning, enabling efficient and precise removal of targeted concepts from a diffusion-based generative model. This section provides supplementary algorithms for our proposed framework, including Algorithm 1 and Algorithm 2.

Algorithm 1 Dynamic Skipping via Interpolation

Require: Total timesteps T, base angles θ_b, all the sample angles θ, each sample angle θ_s, weight factor w_f, noise perturbation $\epsilon \sim \mathcal{N}(0, 1)$, angle threshold θ_{th}, interpolation upper time step t_{upper}, interpolation lower time step t_{lower}, and noise weight factor ϵ_w, $x_t(\theta)$ represents the denoised result at timestep t during the diffusion process, conditioned on the angle θ. At timestep $t = 0$, $x_0(\theta)$ is the final denoised image, and at timestep $t = T$, $x_T(\theta)$ is the noisy image or latent representation.

Examples of base angles:
- 3 base angles: $\theta_b = \{0°, 120°, -120°\}$
- 4 base angles: $\theta_b = \{0°, 90°, -90°, 180°\}$
- 8 base angles: $\theta_b = \{0°, 45°, 90°, 135°, 180°, -135°, -90°, -45°\}$

for each sample angle θ_s **do**
  Compute CLIP similarity $S(\theta_s, \theta_b)$ with key angles
  Select the two most similar key angles as θ_1, θ_2
  Determine skip steps based on threshold and similarity
  Interpolate $x_t(\theta_s)$ from $x_t(\theta_1)$ and $x_t(\theta_2)$ using:
    $x_t(\theta_s) = \lambda x_t(\theta_1) + (1 - \lambda)x_t(\theta_2)$
    $\lambda = \frac{S(\theta_s,\theta_1)}{S(\theta_s,\theta_1)+S(\theta_s,\theta_2)}$
  if $|\theta_s - \theta_b| < \theta_{th}$ **then**
    Use interpolated x_t at $t = T - t_{upper}$
  else
    Use interpolated x_t at $t = T - t_{lower}$
  end if
end for

Description of Algorithm 1: This algorithm accelerates the diffusion process by dynamically skipping denoising steps through interpolation. For each sample-conditioned angle θ_s, it identifies the two most similar base angles θ_1 and θ_2 using a similarity metric (e.g., CLIP similarity). Then, it interpolates the intermediate denoised result $x_t(\theta_s)$ from the known results at θ_1 and θ_2 via a weighted average governed by their similarity scores:

$$x_t(\theta_s) = \lambda x_t(\theta_1) + (1 - \lambda)x_t(\theta_2), \quad \lambda = \frac{S(\theta_s, \theta_1)}{S(\theta_s, \theta_1) + S(\theta_s, \theta_2)}.$$

Depending on whether the sample angle is sufficiently close to a base angle (determined by a threshold θ_{th}), the algorithm either uses the interpolated result at a higher or lower timestep (i.e., fewer or more skipped steps). This allows the system to trade off between fidelity and speed while maintaining semantic consistency.

Algorithm 2 Unlearning via Dynamic Acceleration with Remain and Forget Losses

Require: Pre-trained score network S_t, unlearned model for the target object f_u, fake score network S_f, remain set D_r, unlearn set D_f, override set D_o, all the sample angles θ, each sample angle θ_s, batch size B, weights $\lambda > 0$, $\mu > 0$

Initialize S_f and f_u from pre-trained model
for each epoch **do**
  Sample batch $X_r \sim D_r$, $X_f \sim D_f$, $X_o \sim D_o$
  Call **Algorithm 1** with θ_s ▷ Interpolation Acceleration
  for each sample angle θ_s in θ **do**
    ▷ Train Fake Score Network
    Compute $\mathcal{L}_{fn\text{ remain}}(\theta_s)$
    Compute $\mathcal{L}_{fn\text{ forget}}(\theta_s)$
    Compute total loss: $\mathcal{L}_{fn} = \lambda\mathcal{L}_{fn\text{ remain}} + \mu\mathcal{L}_{fn\text{ forget}}$
    Update S_f using gradient descent on $\mathcal{L}_{fn}$ ▷ λ, μ: weights for remain/forget tasks
    ▷ Train Generator
    Compute $\mathcal{L}_{g\text{ remain}}(\theta_s)$
    Compute $\mathcal{L}_{g\text{ forget}}(\theta_s)$
    Compute total loss: $\mathcal{L}_g = \lambda\mathcal{L}_{g\text{ remain}} + \mu\mathcal{L}_{g\text{ forget}}$
    Update f_u using gradient descent on $\mathcal{L}_g$ ▷ λ, μ: weights for remain/forget tasks
  end for
end for

Description of Algorithm 2: This algorithm presents a training framework for concept unlearning by alternately optimizing the generator and a fake score network using supervision from the remain, forget, and override datasets. A key innovation of this framework lies in the use of dynamic skipping (realized by Algorithm 1) to accelerate the diffusion process for arbitrary sample angles, enabling efficient training while preserving semantic consistency in generated outputs.

At the beginning of each epoch, Algorithm 1 is invoked to perform interpolation sampling across all base angles. This preprocessing step prepares the interpolated denoising results, allowing for fast inference at any sample angle θ_s by reusing the precomputed intermediate states.

Subsequently, the algorithm iterates through all sample angles θ_s defined in the training setup. For each θ_s, it alternates between training the fake score network and the generator. The score network is updated using remain and forget losses to reflect the desired unlearning behavior, while the generator is optimized using the same objectives to remove target concepts while preserving unrelated features.

By integrating dynamic acceleration and angle-wise alternating optimization, this framework achieves fine-grained control over the forgetting process in diffusion models, while significantly reducing the computational burden of full denoising for every training step.

6.2 Dynamic Acceleration Threshold Selection Basis

Recall that in the main paper (see Eq. (10)), we empirically set the angular threshold $\tau = 20^\circ$ to guide the dynamic adjustment of the denoising timestep t_{jump}. Below, we provide supplementary justification for this choice.

Specifically, we precompute and cache intermediate denoising results for a discrete set of reference viewpoints across all sampling steps. For each non-reference training view, we identify its nearest reference angle via cosine similarity and interpolate the cached features at matched time steps to approximate the denoising trajectory. This enables a skip-sampling mechanism in which certain sampling steps are bypassed by reusing spatially coherent representations.

Motivated by the inherent geometric consistency among nearby viewpoints, we hypothesize that smaller angular distances to reference views indicate higher structural similarity and, consequently, greater tolerance for step skipping. Based on this observation, we design a dynamic skipping scheme where the number of skipped steps is conditioned on the angular proximity to the nearest reference angle. In later experiments, we quantitatively assess the trade-off between generation quality and sampling efficiency under this dynamic scheme using SSIM, LPIPS, and ΔPSNR, as well as overall training speedup.

6.2.1 Marginal Benefit Analysis

We introduce the concept of marginal benefit as a key indicator for dynamic acceleration threshold selection.

Combining SSIM decrease and LPIPS increase into a single quality loss metric:

$$\begin{aligned} \Delta Q_{total} &= \alpha \cdot \Delta Q_{SSIM} + \beta \cdot \Delta L_{LPIPS} \\ \text{Marginal Benefit} = \frac{\Delta S}{\Delta Q_{\text{total}}} &= \frac{S_{\text{current}} - S_{\text{previous}}}{\alpha \cdot (Q_{\text{previous}} - Q_{\text{current}}) + \beta \cdot (L_{\text{current}} - L_{\text{previous}})} \end{aligned} \tag{20}$$

- Objective: Find the threshold range that **maximizes** marginal benefit, i.e., achieve the greatest acceleration improvement with the minimal quality degradation.

- Weight coefficients α and β need to be adjusted based on business requirements (defaulting to 0.5 each).

- Physical meaning:

  - $\Delta Q_{SSIM} = Q_{previous} - Q_{current}$ (SSIM decrease, larger value means more quality loss).

  - $\Delta L_{LPIPS} = L_{current} - L_{previous}$ (LPIPS increase, larger value means more perceptual difference).

  - $\Delta S = S_{current} - S_{previous}$ (Speed-up Ratio increase, larger value means faster reasoning).

6.2.2 Experimental Setup and Threshold Determination

To determine the optimal dynamic acceleration threshold, we sampled 36 viewpoints within the $[0°, 45°]$ range from the base view at $2°$ intervals, using 4 reference views. Experiments were conducted on the Yellow Car unlearning task. For each candidate threshold, we computed SSIM, LPIPS, and acceleration ratio under the dynamic 4-view, 12-step sampling configuration, and subsequently calculated the marginal benefit. The angle yielding the highest marginal benefit was selected as the optimal dynamic threshold. As shown in Figure 4a, the marginal benefit peaks at a threshold of $20°$.

To further validate the effectiveness of the proposed dynamic strategy, we compared it with a static configuration using 4 reference views and 12 uniform steps, without threshold adaptation. This comparison demonstrates that our strategy can achieve acceleration while maintaining high generation quality. The results of this comparative experiment are presented in Figure 4b.

From the figure, we observed that as the angular threshold increases from $0°$ to $45°$, the SSIM decreases from 0.69 to 0.51, while LPIPS increases from 0.05 to 0.36, indicating a consistent trade-off between fidelity and efficiency. Meanwhile, the acceleration ratio improves from the static baseline of 0.29 up to 0.48. Notably, the $20°$ threshold yields a balanced performance—achieving 0.62 SSIM, 0.22 LPIPS, and 0.38 acceleration ratio—and represents the optimal marginal gain point. Beyond $20°$, marginal returns diminish: from $20°$ to $30°$, acceleration increases only 0.06, while LPIPS worsens 0.07. After $30°$, visual degradation accelerates, with LPIPS exceeding 0.3 and SSIM dropping below 0.6. These results confirm that moderate thresholds (approximately $20°$) achieve the best trade-off, while aggressive skipping leads to diminishing quality returns.

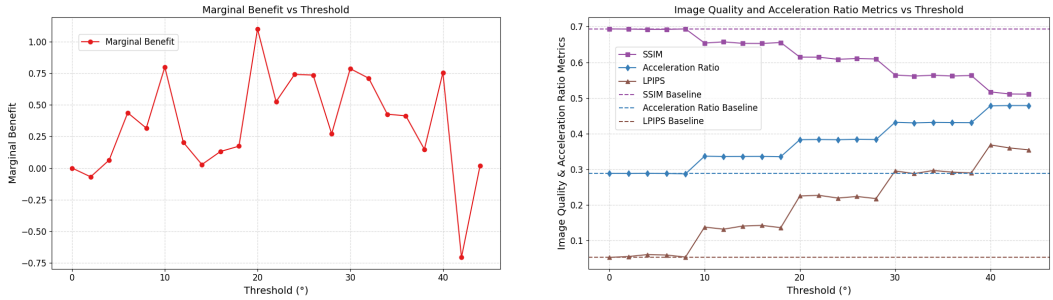

(a) Marginal benefit vs. threshold angle.

(b) Comparison between dynamic and static strategies.

Figure 4: Analysis of threshold selection and strategy comparison.

7 Supplementary Experimental Results

7.1 Experimental Settings

Implementation Details

To cover the full 360° horizontal field of view, we define the angular range as $(-180°, 180°]$. Given the desired number of reference directions $N_{\text{reference}}$, we generate a set of reference angles starting from $0°$ with a fixed interval of $360°/N_{\text{reference}}$. As these angles are initially defined in the $[0°, 360°)$ range, we map them into $(-180°, 180°]$ to align with the defined coordinate system.

During the training stage of the unlearning task, we additionally sample one angle every $10°$ over the range from $-180°$ to $180°$, excluding the reference angles. This ensures dense and uniform coverage across the entire horizontal span. Such a setup helps the model generalize to diverse viewpoints while maintaining consistency between the training and evaluation angular distributions.

Hyper-parameter Settings

In all experiments, we employ the Adam optimizer, where β_1 and β_2 denote the exponential decay rates for the first and second moment estimates, respectively. The parameters λ and μ represent the regularization coefficients used in the objective function. The term ϵ_t denotes the standard Gaussian noise added during the diffusion process at time step t, with $\epsilon_t \sim \mathcal{N}(0, 1)$.

The *Number of References* represents the number of pre-cached reference angles used for subsequent interpolation to estimate noise; the *Skip Steps* indicates the initial steps skipped during the sampling process.

Table 3: Hyperparameters for Fake Score and Generator

Parameter	**Fake Score**	**Generator**
λ	1.0	1.0
μ	0.01	0.01
Optimizer	Adam	Adam
Learning Rate	4×10^{-6}	6×10^{-6}
β_1	0.0	0.0
β_2	0.999	0.999
ϵ_t	10^{-8}	10^{-8}

Table 4: Experimental Settings for Different Reference Angles and Unlearn Effects

Parameter	Reference Angles Experiment	Target Forget Images Experiment
GPU	NVIDIA A100 80GB	NVIDIA A6000 48GB
Batch Size	8	2
Sample Steps	32	32
Training Epochs	5	-
Number of References	-	4
Skip Steps	-	12

7.2 Multi-angle presentation of the results from the main experiment

We provide additional experimental results to supplement the main paper. The following provides concrete examples of the unlearning implementation for the retargeting, stylization, and partial tasks in our experiments.

Table 5: Representative application cases categorized by type.

Category	Case Examples
Style Transfer	Yellow Car Transformation, Metal Style Ice-cream Transformation, Bronze Statue Transformation
Whole Object Retarget	Cherry to Banana, Barrier to Fire Hydrant, Football to Phone
Partial Edit Replacement	Barrel Add Black Lid, Doraemon with Hat, Minion with Backpack, Stool with Pot

Unlearning task 1: Style Transfer

- **Yellow Car Transformation**: In this experimental setup, a frontal image of a *silver car* is designated as the *forget image*, representing the category to be unlearned, while a frontal image of a *yellow car* which is generated by adjusting the color tone of the original image, changing the car body color to yellow while keeping other visual content unchanged, serves as the *override image*, representing the target category. During training, the *forget image* combined with a given *sample angle* is replaced by the *override image* with the same corresponding *sample angle*. This configuration aims to evaluate the model's ability to forget and override when the object's appearance attributes, such as color, change.
- **Metal Style Ice-cream Transformation**: The forget image is a Green ice cream cone, while the override image is generated by changing the color of the ice cream to a metallic sheen. Similar to the Yellow Car Transformation case, both the forget angle and the override angle are aligned with the sample angle.
- **Bronze Statue Transformation**: The forget image is a white marble sculpture, while the override image is generated by changing the color of the sculpture to bronze. Again, both the forget angle and the override angle are aligned with the sample angle.

Unlearning task 2: Whole Object Retarget

- **Cherry to Banana**: In this experimental setup, a frontal image of a *cherry* is designated as the *forget image*, representing the category to be unlearned, while a frontal image of a *banana* serves as the *override image*, representing the target category. During training, the *forget image* combined with a given *sample angle* is replaced by the *override image* with the same corresponding *sample angle*. This configuration is designed to evaluate the model's capability in performing semantic transformation between different object categories.
- **Barrier to Fire Hydrant**: The forget image is a barrier, while the override image is a fire hydrant. Similar to the Cherry to Banana case, both the forget angle and override angle are aligned with the sample angle.
- **Football to Phone**: The forget image is a football, while the override image is a phone. Again, both the forget angle and override angle are aligned with the sample angle.

Unlearning task 3: Partial Edit Replacement

- **Minion With Backpack** This setting aims to evaluate the model's response to viewpoint variations and additional attribute modifications. The *forget image* is a frontal view of a minion. When the *sample angle* lies within the range $[-90°, 90°]$, the *override image* is the same as the *forget image*, and both the *forget angle* and *override angle* match the *sample angle*. However, when the *sample angle* falls outside this range (i.e., side or rear views), the *override image* is replaced by a rear view of the minion wearing a red backpack, and the *override angle* is defined as the *sample angle* plus $180°$ (i.e., the opposite viewing direction). This setting simulates the unlearning and rewriting behavior when the target object undergoes structural or appearance changes under different viewpoints. The specific angle relationships are as follows:

  - If the original *forget angle* is within $[-90°, 90°]$, the guidance condition uses the original *forget image* and *forget angle*.
  - If the *forget angle* lies in $[-180°, -90°)$, the guidance condition replaces the image with the *override image* and adjusts the angle to *forget angle* plus $180°$.
  - If the *forget angle* lies in $(90°, 180°]$, the guidance condition replaces the image with the *override image* and adjusts the angle to *forget angle* minus $180°$.

- **Barrel Add Black Lid**: The forget image is a wooden barrel, while the override image is generated by adding a big black lid to the original barrel. Both the forget angle and the override angle are aligned with the sample angle.

- **Doraemon With Hat**: The forget image is a Doraemon, while the override image is generated by putting a red cap on Doraemon's head.. Both the forget angle and the override angle are aligned with the sample angle.

- **Stool With Pot**: The forget image is a wooden stool, while the override image is generated by placing a small plant in a pot on the stool. Again, both the forget angle and override angle are aligned with the sample angle.

Figure 5 presents multi-view visualizations of the unlearning outcomes for various target objects across multiple categories, demonstrating the consistency and robustness of the unlearning effect under different viewing angles.

In each row, the left-most pair shows the original source object (left) and the desired unlearned target (right). The right panel visualizes the unlearned results rendered from multiple canonical perspectives (front, side, back, etc.). It can be observed that across diverse object types—including vehicles, statues, characters, and everyday items—the model consistently applies unlearning effects to generate novel outputs aligned with the desired target identity or semantics. For instance, the "car" is reliably altered to resemble a yellow sports model across all views, while the "Doraemon" character is consistently altered to wear a red hat across all viewpoints, suggesting strong disentanglement and generalization capacity in the forgetting process.

These results validate that our method does not overfit to a single viewpoint, but achieves semantically coherent forgetting across multiple 3D-consistent renderings, highlighting the model's capacity for multi-perspective semantic consistency in unlearning tasks.

Figure 5: Demonstration of multi-perspective effects on the forget set for different unlearning tasks.

7.3 3D Reconstruction Demonstrations

7.3.1 Qualitative Results of 3D Unlearning

We showcase 3D reconstruction results for several tasks, presenting pairs of rendered images and depth maps.These results demonstrate that our unlearning strategy not only performs effectively in multi-view consistency settings but also extends to full 3D geometry. Specifically, we observe consistent suppression of undesired concepts across different viewpoints and depth cues, indicating that unlearning has been successfully integrated into the volumetric representation. This highlights the generalizability and spatial coherence of our method beyond view-based supervision, ensuring that undesired features are removed holistically rather than superficially.

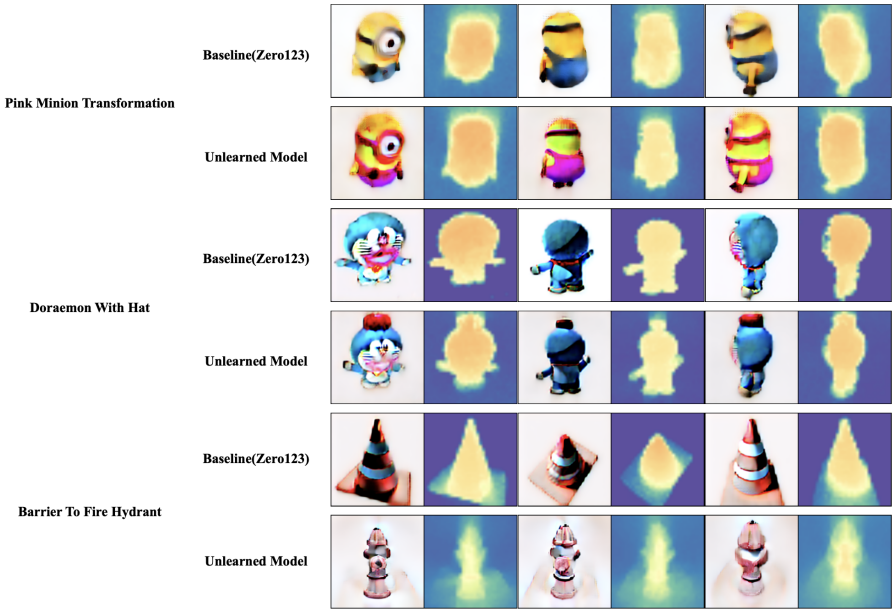

Figure 6: Qualitative 3D reconstruction results across different tasks after unlearning.

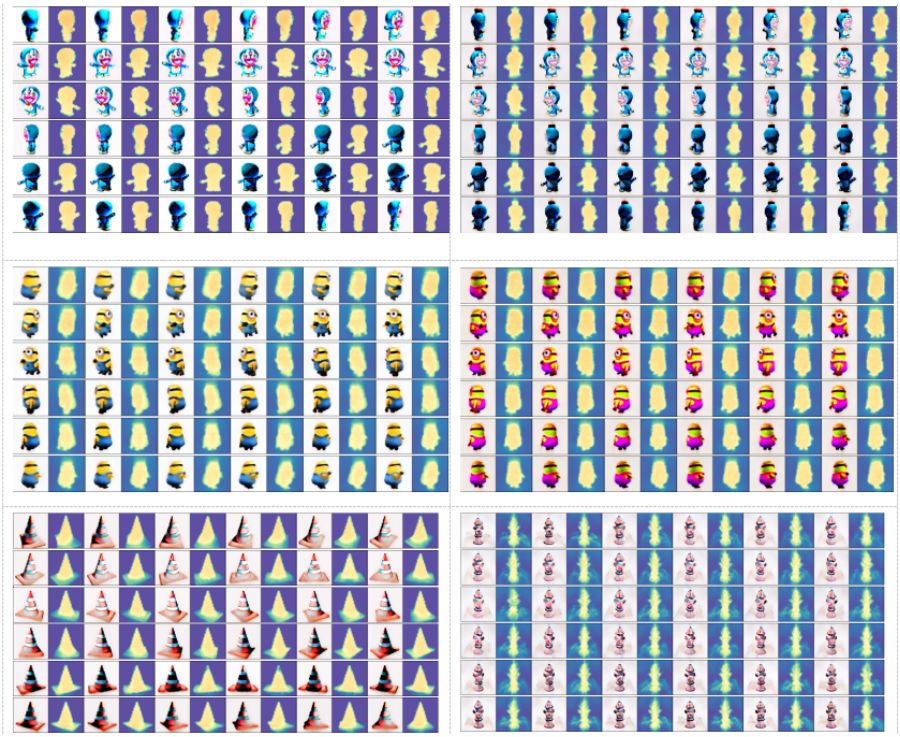

Figure 7: more angles sampled in 3D rec

7.3.2 Results on Free3D Framework

To demonstrate the generalizability of our dynamic skipping framework beyond Zero123, we integrate it with Free3D, a state-of-the-art diffusion-based 3D generation model. Our method is adapted by aligning the multi-view conditioning and applying the view-consistent acceleration strategy during the denoising process.

Figure 8: Multi-view 3D generation results using Free3D integrated with our dynamic skipping framework. **Leftmost column:** Input view. **Remaining columns:** Generated novel views from different angles. The high consistency and quality across views demonstrate the effectiveness and generalizability of our method on the Free3D architecture.

Figure 8 shows multi-view renderings of 3D objects generated by Free3D enhanced with our dynamic skipping approach. Each row presents a different object reconstructed from a single input view (shown on the left), with subsequent columns showing synthesized views from novel angles. The results exhibit high visual fidelity, geometric consistency, and smooth transitions across viewpoints, confirming that our acceleration framework is effective in improving inference efficiency while preserving generation quality on diverse 3D diffusion architectures.

This successful integration underscores the flexibility and broad applicability of our method, positioning it as a promising general acceleration paradigm for multi-view 3D generation systems.

7.4 Effect of View-consistent Acceleration without Unlearning

To isolate the effect of acceleration from unlearning, we conduct an ablation study on the Zero123 baseline by applying our multi-view consistency-guided acceleration without any unlearning objective. Specifically, we introduce skip-step sampling with different reference view counts (3/4/8 views) to observe how generation quality changes purely due to acceleration.

Table 6 reports the ΔFID scores, computed as the difference between the FID of accelerated models and the baseline Zero-1-to-3 model. Positive values indicate improved fidelity relative to the baseline, while negative values indicate a degradation.

Table 6: Δ FID Comparison between Accelerated Models and Baseline (Zero-1-to-3).

Method	Steps Skipped	Delta FID
3 View	8	+0.9779
	12	-6.7059
	16	-15.8247
4 View	8	+0.3379
	12	-7.1140
	16	-34.8952
8 View	8	+2.8421
	12	-10.5640
	16	-74.9905

Table 7: Generation Quality Metrics under Different Dynamic Skipping and Reference Views Configurations on Zero123.

Metrics	**SSIM**	**LPIPS**	**PSNR**	**MSE**
zero123	0.7469	0.2526	13.53	0.0597
3view 8skip	0.7683	0.2417	14.29	0.0494
3view 12skip	0.7641	0.2463	14.17	0.0507
3view 16skip	0.7605	0.2532	14.04	0.0532
4view 8skip	0.7728	0.2389	14.34	0.0424
4view 12skip	0.7701	0.2418	14.27	0.0441
4view 16skip	0.7674	0.2485	14.13	0.0511
8view 8skip	0.7672	0.2331	14.57	0.0467
8view 12skip	0.7643	0.2338	14.51	0.0483
8view 16skip	0.7614	0.2515	14.41	0.0487

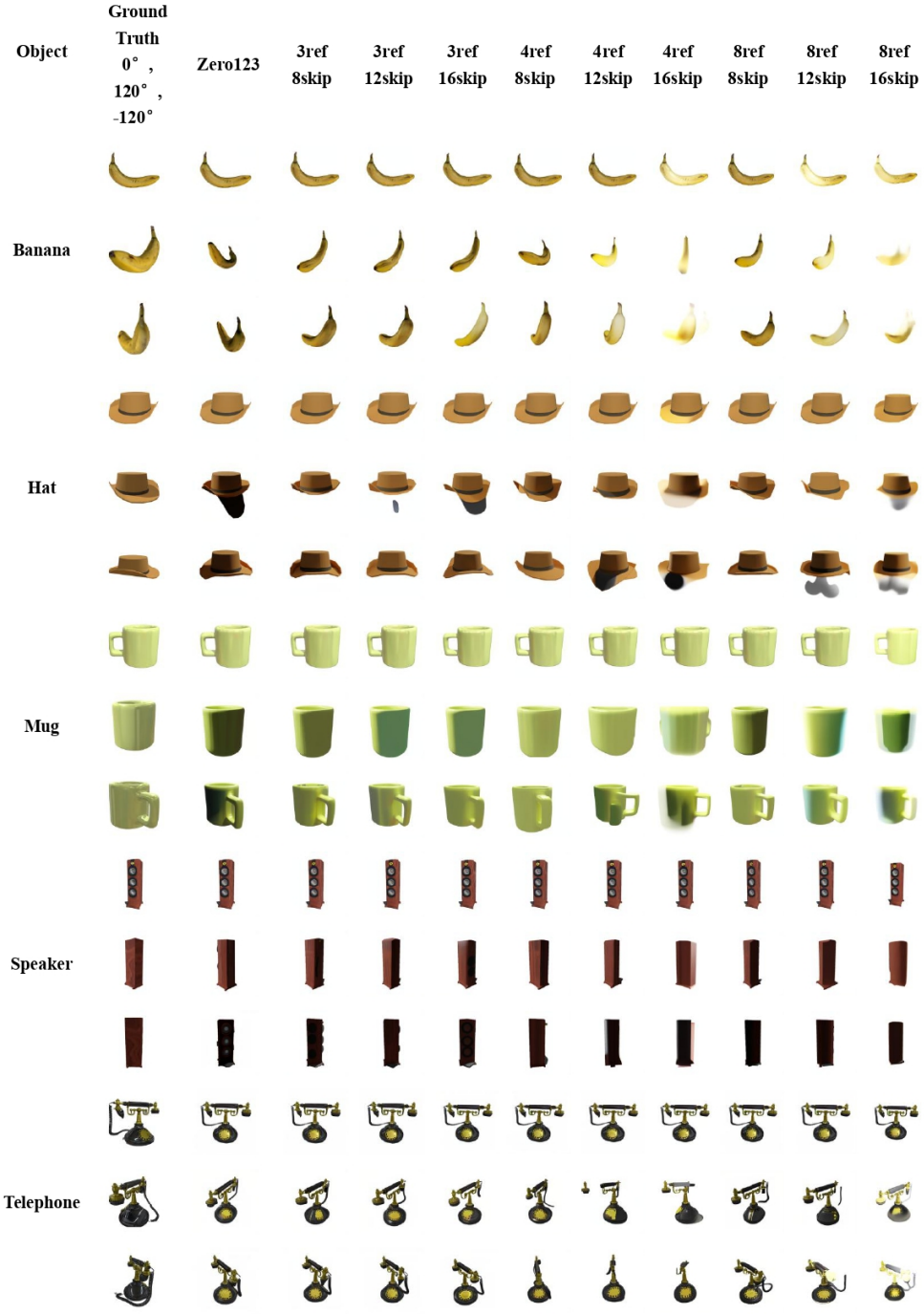

Figure 9: Qualitative results demonstrating the effect of view-consistent acceleration without unlearning. (Corresponds to Table 6 data)

We analyze the results from two perspectives: the number of reference (baseline) views used for interpolation, and the number of diffusion steps skipped during inference.

Effect of Reference View Number: When fixing the number of skipped steps, increasing the number of reference views generally leads to a more accurate initialization for the diffusion process due to finer angular coverage and closer interpolation points. This advantage is reflected in the 8-step skip setting, where the model with 8 reference views achieves the highest positive ΔFID (+2.8421), compared to 3 and 4 views (+0.9779 and +0.3379 respectively). This suggests that a denser set of baseline views provides a better starting point, facilitating high-fidelity multi-view synthesis.

Effect of Skipped Diffusion Steps: Across all reference view counts, increasing the number of skipped diffusion steps significantly degrades performance. For example, under 8 reference views, the Delta FID drops from +2.8421 at 8 skipped steps to -10.5640 at 12 skipped steps and further to -74.9905 at 16 skipped steps. This trend indicates that while skipping steps can accelerate inference, excessive step skipping undermines the model's ability to refine the initial interpolated latent, leading to poorer image quality.

Interaction between Reference Views and Skipped Steps: Interestingly, the degradation caused by skipping more steps is more pronounced as the number of reference views increases. This is likely because the interpolation between two nearby reference views produces a finer but potentially more complex latent initialization that requires sufficient diffusion steps to properly refine. When too many steps are skipped, the model lacks the capacity to adequately recover details and enforce multi-view consistency, resulting in a sharper performance drop.

Qualitative results illustrating these effects are shown in Figure 9.

7.5 Inference Efficiency

As shown in Table 8, the baseline represents the time (1.1000 seconds) taken by Zero123 to sample an image without using dynamic skipping via interpolation. The other columns show the sampling times with different skip steps, along with the speedup ratios compared to the baseline.

Table 8: Inference Time and Speedup of Dynamic Skipping Strategies.

Method	Full Sample (s)	Skip 8 Sample (s)	Skip 12 Sample (s)	Skip 16 Sample (s)
Baseline (No Accelerate)	1.1000	-	-	-
Accelerated (Skip 8)	1.1000	0.7709	-	-
Accelerated (Skip 12)	1.1000	-	0.6459	-
Accelerated (Skip 16)	1.1000	-	-	0.5193
Speedup (vs. Baseline)	-	1.4286	1.7072	2.1210

The speedup ratios are calculated as $\text{Speedup} = \frac{\text{Baseline Time}}{\text{Accelerated Time}}$. Results show that skipping 8, 12, and 16 steps achieves $1.43\times$, $1.71\times$, and $2.12\times$ faster inference, respectively, demonstrating the efficiency of our dynamic skipping strategy.

8 Limitation and Social Impact

While our method introduces a novel framework for machine unlearning in 3D generation, several limitations remain. We categorize these into technical limitations and broader societal concerns, and outline promising future directions to address them.

Technical Limitations.

- **Model Generalization.** Our framework is currently validated on Zero123 and Zero123XL. Its applicability to other 3D generation paradigms (e.g., NeRFs, mesh-based models, point-based representations) remains untested and may require architectural adaptations.
- **View Similarity Estimation.** The dynamic skipping mechanism leverages CLIP-based similarity to approximate view-level correspondence. While practical, this may be suboptimal for objects with subtle geometric or structural variations that CLIP embeddings cannot fully capture.

- **Manual Target Selection.** The forget/remain/retarget sets are manually specified. Real-world deployment would benefit from automatic identification of privacy-sensitive or biased content, requiring new detection or attribution tools.
- **Hyperparameter Sensitivity.** Our method depends on empirically chosen parameters, such as the angular threshold τ and skip-step schedule. These may require retuning on new datasets or under different acceleration regimes.
- **Lack of Robustness Evaluation.** We do not assess the robustness of the unlearned model against adversarial attacks such as model inversion, concept re-injection, or prompt-based data recovery.

Future Work.

- **Broader Model Applicability.** We aim to adapt our framework to a wider range of 3D generation backbones, including volumetric NeRFs, implicit surfaces, and real-time rendering architectures.
- **Privacy-Aware Target Detection.** Future work will explore integrating privacy or attribution detectors to automatically identify sensitive content for targeted unlearning without human intervention.
- **Unlearning Without Retargeting.** While our method currently aligns forgotten content with a retargeted distribution, we plan to investigate pure erasure techniques without replacement, suitable for content removal rather than transformation.
- **Online and Continual Unlearning.** Extending our method to dynamic settings—such as continual learning or post-deployment unlearning requests—is an important direction for practical applications.
- **Trustworthy Unlearning Evaluation.** We plan to develop formal verification protocols and benchmarks to quantify the effectiveness and irreversibility of unlearning across diverse tasks and threat models.

Social Impact Considerations. Our framework raises potential concerns regarding privacy leakage and model bias, especially in the context of modular or pre-trained model reuse.

- **Privacy Risk.** By reusing pretrained parameters, the unlearned model may unintentionally retain latent traces of upstream data. Adversaries could potentially reconstruct sensitive content through model inversion or prompt tuning. One mitigation strategy is to increase the diversity and number of pretrained models used, ensuring that no single model contains sufficient information to recover sensitive content.
- **Model Bias.** Biases present in the original training data or source models may propagate through the unlearning process. To mitigate this, we propose diversifying the source model pool and introducing diversity-promoting regularization during training. This helps prevent over-reliance on any single biased component and encourages fairer predictions.

We consider these directions essential for improving the robustness, fairness, and ethical deployment of 3D unlearning systems, and plan to extend our study to address these limitations in future iterations of this research.